Title: General characterization of regeneration in *Aeolosoma viride*

Authors: Chiao-Ping Chen[1†], Sheridan Ke-Wing Fok[1†], Yu-Wen Hsieh[2], Cheng-Yi Chen[3], Fei-Man Hsu[4] and Jiun-Hong Chen[1*]

Affiliations:

[1]Department of Life Science, National Taiwan University, Taipei, Taiwan

[2] Max Planck Institute of Molecular Cell Biology and Genetics, Dresden, Germany

[3] Stowers Institute for Medical Research, Missouri, America

[4] Graduate School of Frontier Sciences, The University of Tokyo, Chiba, Japan

*Corresponding author:

Development of Life Science

National Taiwan University

Taipei, 106

Telephone: +886 (2) 33662502

E-mail: chenjh@ntu.edu.tw

[†] Chiao-Ping Chen and Sheridan Ke-Wing Fok are co-first authors of this paper.

Abstract

Regeneration has long attracted scientists for its potential to restore lost, damaged or aged tissues and organs. A wide range of studies have conducted on different model organisms on both cellular and molecular levels. Current evidences suggest that a variety of regenerative strategies are developed and used by different species, and their regenerative strategies are highly correlated to their reproductive methods. Our

present work focused on the freshwater annelid *Aeolosoma viride*, which reproduces by paratonic fission and is capable of complete regeneration. We found out that *A. viride* can regenerate both anterior and posterior end, even with only 3 segments remained. This process is characterized by epimorphosis that involves large amount of cell proliferation which drives the formation of blastema. Cell proliferation and regeneration successful ratio were significantly decreased when treated with microtubule inhibitor taxol or *Avi-tubulin* dsRNA, which confirmed that cell proliferation served as a key event during regeneration. Together, our data described the regenerative processes of *A. viride*, which includes high level of cell proliferation and the formation of blastema. Furthermore, our findings demonstrated *A. viride* as a potential model for the study of regeneration.

Keywords: *Aeolosoma viride*, Epimorphic regeneration, Cell proliferation, Blastema

Introduction

An ability to regenerate lost body part is widely, but non-uniformly, distributed in the animal kingdom [1-3]. Both the capacities and mechanisms of regeneration differ between taxa. T. H. Morgan described the processes of regeneration in two generalized terms, namely morphallaxis and epimorphosis [4]. Morphallaxis is

43 characterized by rearrangement of pre-existing cells and the absence of blastema [5].
44 Early regeneration in hydra is a classic example of morphallaxis as it requires
45 minimum cell proliferation and redistribution of pre-existing tissues. In epimorphosis,
46 on the other hand, undifferentiated cells or progenitor cells aggregate at the wound
47 sites, and these undifferentiated cells proliferate to form a blastema [6, 7]. Therefore,
48 cell proliferation is required for epimorphic regeneration, and application of drugs that
49 perturb cell cycle progression, such as nodcodazole or hydroxyurea, would prevent
50 normal progression of regeneration [8].
51
52 Asexual reproduction is often compared to regeneration, since identical individuals
53 arise from fragments of somatic tissue in both processes [9]. Asexual reproduction in
54 annelids can be divided into two major types: architomy and paratomy. Architomy is
55 fission followed by fragmentation. Contrarily, paratomy required individuals to be
56 fully formed or developed prior to fission [10]. In paratomic reproduction,
57 reconstitution or rearrangement of somatic tissue typically occurs in a predictable
58 growth zone. Previous studies demonstrated that such a growth zones can also
59 regenerate lost body parts after injury in certain species reproduce by paratomic
60 fission [9, 11].
61

62 Paratomic fission has been described as a common character of annelids, as it is found
63 in taxanomic groups such as Sipuncula, Serpulidae, Aeolosomatidae, and Naididae
64 [12]. Regeneration is also wide-spreading among annelids [13, 14]. Nevertheless,
65 species differs in their regenerative capacities. For example, the naidid *Pristina leidyi*
66 mostly reproduce by paratomic fission and is able to complete both anterior and
67 posterior regeneration [11]. In contrast, the capitellid polychaete *Capitella teleta*
68 mostly reproduce sexually and is only capable to partially regenerate its posterior end
69 [15]. Such a difference may reflect a connection between asexual reproduction by
70 paratomic fission and regeneration [9, 12, 16].
71
72 Aeolosomatidae are polychetae that mostly inhabit in fresh water environment [17].
73 Approximately 30 species have been identified in this family, and predominantly
74 reproduce by agametic reproduction [10, 18]. Most aeolosomatid species reproduce
75 by paratomic fission to create clonal individuals, and an ability to regenerate the
76 anterior and posterior segments after injury has been demonstrated in some species of
77 this family [19]. However, there is no detailed descriptive characterization of the
78 regeneration in this group of annelids. In this study, we provided a detailed
79 description of the regeneration process in *Aeolosoma viride*. It was observed that this
80 worm can restore its lost body parts, both anteriorly and posteriorly, within 3-5 days.

Furthermore, we demonstrated that a high level of cell proliferation occurs at the wound site and that such a cell proliferation activity is critical for the completion of regeneration. Using pulse-and-chase experiments, we were able to show that cell migration has no particular role in anterior regeneration of *A. viride*. Finally, our study demonstrated the potential of *A. viride* to be an excellent model for regenerative studies.

Results

General and reproductive characteristics of *A. viride*

Aeolosoma viride is a 2-3 mm length semi-transparent annelid contained 10 to 12 segments with pairs of chaetae at each side of the worms. The intact worm has a ring-like mouth structure that can be observed at both dorsal and ventral side of the peristomium (1st segment). Mouth is connected to an enlarged digestive tract located at the center of the worm, which can be easily observed under a dissecting microscope. *A. viride* exclusively perform paratonic fission to asexually reproduce one progeny from its posterior end (Fig. 1). The paratonic fission started by extension of the posterior end. Worms exceeding 12 segments with an unusual lengthy posterior region could be easily observed (Fig. 1C). The anterior portion of the offspring gradually developed and formed a head shape tilted apart from the parental worm (Fig. 1D). At

this stage, the parent and the progeny can be easily distinguished. Finally, the offspring worm separates apart from the parental worm, and becomes an individual worm (Fig. 1E).

Anterior regeneration in *A. viride*

Anterior amputation is performed in front of the enlarged digestive tract. Immediately after amputation, the worm severely twisted; fluids and food residues gushed from the inner cavity. At 3 hours post amputation (hpa), the regenerating *A. viride* adhered on the bottom of culture chamber, and its wounded area remained rough and uneven. The rough wounded area became smoothened within 6 hpa. At 12 hpa, a small amount of tissue became lighter and clearer in color, started to develop at the regenerating area. This tissue will later be proven to be the regenerative blastema. The protruding regenerative blastema expanded from the center of the wounded area and became apparent from 24 to 48 hpa. Vertical contraction could be observed from 72 hpa, but the regenerating worms were still unable to move freely. The reappearance of ring-like structure characterized mouth formation, and a tubular structure (esophagus) extended to connect with the enlarged digestive tract at 96 hpa. After 96 hours of regeneration, the regenerating head area gradually bulged and became wider than other body segments. The prostomium expanded from 96 to 120 hpa (Fig. 2B).

During the entire process of regeneration, the regenerating *A. viride* remain adhere on the bottom of culture chamber. Most of them could swim freely around 120 hpa, which was considered as an indicator for successful regeneration in *A. viride*.

The regenerative capacity of *A. viride*

For characterization of the regenerative capacity, either the anterior or the posterior ends of worms were amputated. Amputated worms with three segments could still complete regeneration, even the successful ratio was around 40%. Over 60% of worms with 6 or 9 posterior segments completed their anterior regeneration at 5 day post amputation (dpa) (Fig. 3). Posterior regeneration shared a similar pattern. Over 53.3% worms with three anterior segments completed their posterior regeneration. Worms with 6 or 9 anterior segments increased successful ratio of posterior regeneration over 80% at 3 dpa (Fig. 3). Since the anterior segments of *A. viride* contain the mouth and the brain, their complexity and importance outweigh the posterior segments. Therefore, all following experiments in this study were conducted on the anterior end.

Cell proliferation in the regenerative process of *A. viride*

EdU signal showed proliferating cells continuously present in *A. viride*. The worms

were also stained with a nuclear dye Hoechst 33342 to conform the EdU labeling (Fig. 4A). Intact and regenerating worms were incubated in EdU solution 12 hours prior to fixation. Normally, the EdU^+ cells were significally detected at the posterior end of intact worm, the area of asexual reproductive zone, which is the connecting interface between the parent and the future offspring. The EdU signal was also detected at the anterior mouth with minor EdU signals randomly distributed in intact and regenerating worms from 0 to 12 hpa. However, signals posterior to the amputation site quickly diminished after 24 hpa. During regeneration, the EdU signal became concentrated at the regenerating blastema, and the strongest signal was observed at 24 and 48 hpa, then gently decreased from 72 to 120 hpa. At 96 and 120 hpa, EdU^+ cell formed a ring-like shape at the center of head, which indicated the development of mouth in the regenerating worms (Fig. 4C).

Cell proliferation is required for anterior regeneration

Aeolosoma viride were treated with taxol, an inhibitor of cell proliferation that works by interfering with the normal function of microtubules. As previous result has shown, the largest amount of proliferating cells was detected at 48 hpa (Fig. 4C). However, the EdU signal in the blastema were apparently reduced by 25 μM of taxol at 48 hpa, which indicated that the proliferating blastema was not properly formed at anterior

157 regenerating site (Fig. 5A). The regeneration successful ratio of *A. viride* treated with
158 25 μM taxol decreased 80% at 5 dpa and 45% at 7 dpa (Fig. 5B). Also, the bulged
159 head of the regenerating *A. viride* was absent after taxol treatment, and only a tiny
160 blastema was observed at 5 and 7 dpa (Fig. 5C).
161
162 To confirm the importance of cell proliferation on regeneration in *A. viride*, we also
163 used gene-specific dsRNA to perform RNA interference. Both feeding and
164 microinjecting dsRNA successfully reduced the expression of *Avi-tubulin* mRNA by
165 50% compared to *yfp* dsRNA (MOCK) (Fig. 6A). Western blot was conducted to
166 further confirm this result. The predicted molecular weight of tubulin protein is 48.8
167 kDa. *Avi*-actin served as loading control, and its predicted molecular weight is 42.1
168 kDa. The result showed a significant reduction of tubulin protein expression
169 comparing to MOCK RNAi (Fig. 6B). In addition, worms treated with *yfp* dsRNA
170 regenerated normally. But, the regeneration of *Avi-tubulin* RNAi treated animals was
171 significantly inhibited at 5 dpa. The group of feeding dsRNA reduced successful ratio
172 of regeneration by 45%, whereas the group of injecting dsRNA reduced by 35% (Fig.
173 6C).
174
175 **Cell migration in the regeneration of *A. viride***

176 Some speculated that the source of stem or progenitor cells in the regenerative area
177 could be migration [20]. Stem cell migration not only is fundamental to embryonic
178 development, but also indispensable to adult tissue homoeostasis and repair [21].
179
180 To examine the role and importance of cell migration during anterior regeneration of
181 *A. viride*, pulse-chase experiment with EdU labeling was performed. Only a few EdU^+
182 cells were detected at the surface of the newly regenerated tissue at 24, 72 and 120
183 hpa (Fig. 7). However, the distribution of EdU^+ cells around non-regenerated area was
184 evident from 24 to 120 hpa.
185
186 **Discussion**
187 *Aeolosoma viride* is the first species in Aeolosomatidae used as a model for detailed
188 regeneration study. In this study, we had carefully evaluated the regenerative capacity
189 of *A. viride*. Regeneration of *A. viride* followed by either anterior and posterior
190 amputation could be completely restored within 5 days and 3 days respectively. Most
191 worms could survive and regenerate with 3 segments. Anterior regeneration showed
192 lower successful ratio than posterior regeneration. It is reasonable to explain that the
193 anterior regeneration is involved the restoration of a more complex structure including
194 head and mouth. Even so, compared with earthworm *Enchytraeus japonensis* that

195 could regenerate into complete individual from 6 fragments [22], and *Eisenia fetida*
196 that could only partially regenerate [23], *A. viride* clearly demonstrated a stronger
197 regenerative ability.
198
199 Sexual and asexual reproduction including budding, paratonic fission, and
200 fragmentation have all been documented in annelid reproduction [24]. Previous study
201 has recorded the regenerative capacity and reproductive strategies of many annelids,
202 and discovered that most annelids capable of head regeneration reproduce by asexual
203 reproduction [25]. *Aeolosoma viride* had been recorded that its reproduction is
204 exclusively asexual by paratonic fission [18]. Our study provided detailed imaging on
205 the entire process, and confirmed the idea that animals with asexual reproductive
206 characters typically demonstrated strong regenerative capacity.
207
208 Cell proliferation is generally considered to be the key event that occurs at the area of
209 regeneration [26, 27]. The contribution of cell proliferation to regeneration differs
210 across metazoan models [8]. In this study, large amount of EdU^+ cells present at
211 blastema during regeneration. Combined with the changes in morphology, we
212 observed that anterior amputation in *A. viride* is followed by the formation of
213 blastema with great quantity of cell proliferation during regeneration. Also, significant

214 decrease of proliferating cells was observed at the blastema after treated with mitotic
215 inhibitor taxol. Together, these data demonstrated the importance of cell proliferation
216 in the regenerative process of *A. viride*.
217
218 Although variation exists in regeneration ability and mechanism, the widespread
219 phylogenetic distribution of blastema formation in annelid suggested an evolutionary
220 ancient origin of regeneration process. Even though, recent studies indicated that
221 regeneration could not be solely classified as epimorphic or morphollatic, several
222 segmented worm species including *Branchiomma luctuosum* and *C. teleta* have
223 shown limited evidence for morphallaxis [28, 29]. Morphallaxis is characterized by
224 rearrangement of pre-existing tissues, which strongly depend on stem cells or
225 remaining undifferentiated cells migrating to the injured site [30]. Our data supported
226 the hypothesis that *A. viride* carried out anterior regeneration by epimorphosis which
227 is consistent with most other annelids [29, 31-34]. Recent findings inferred that
228 regeneration in annelids involves both cell proliferation and cell migration [35]. And
229 the cellular source of blastema originated from the migration of stem cells [20].
230 According to our pulse-chase experiment, EdU^+ cells were limited in the anterior
231 regenerating site, which means that only a small amount of proliferating cells
232 migrated into the wounded area during anterior regeneration. This allowed us to

hypothesize that cell migration served no specific or limited role during anterior regeneration in *A. viride*. There was no evident morphallaxis occurred, however, further experiment with stem cell markers and live-imaging are needed for a definite conclusion.

Limited regeneration studies conducted on annelids model organisms. Hydra and planarian are both considered as the master of regeneration, and often used as the model organisms for regeneration studies [7, 36-39]. But, there are specific restrictions on regeneration studies regarding these commonly used animals. Both planarian and hydra lack sophisticated organ systems and a complex central nervous system, which is far different from vertebrate animals. Hydra regeneration is also classified as morphallatic, which means that they could regenerate under limited cell proliferation [40, 41]. And based on current studies, none of the known vertebrate could regenerate mainly through morphallaxis. Epimorphosis is the major type of regeneration observed in vertebrate animals. Salamander, *Xenopus* and zebrafish are all prominent examples of animal models used in the study of epimorphic regeneration. However, regeneration in these animals is limited to specific organs or tissues. Some might even have restriction on early stage of life [42-44]. Certain species of echinoderms could completely regenerate from a piece of tissues [45], but

252 echinoderm shared very different characteristic from vertebrate animals, such as body
253 symmetry, lack of head, digestive, and circulatory system. Due to the limitations that
254 current models retained, we believe that annelids can serve as different model
255 organism for the study of regeneration. Besides an evolutionary advantage, *A. viride*
256 also possess similar level of experimental advantages compare to many current model
257 organisms. Small molecular inhibitors, molecular tools were both applicable on this
258 worm. First, *A. viride* is easy to maintain and raise in laboratory. Second, *A. viride* has
259 small and transparent body which make them easy to be manipulated and observed
260 during the experimental processes. Last but not least, RNA interference was used in
261 the study of molecular biology to knock down or silence specific mRNA expression.
262 Feeding method commonly designed for *C. elegans* and microinjecting method
263 designed for animal embryo and adult were both functional in this newly introduced
264 model animal [46]. In addition to its regeneration capacity, this small annelid has
265 relative short lifespan and reproductive cycle which is suited for study on aging
266 [47-49].
267
268 In conclusion, we examined the regenerative capacity in *A. viride*, especially on
269 anterior regeneration. In addition to strong regeneration ability, *A. viride* has several
270 characters that may make them valuable as a potential animal model for regeneration

271 research.

272

273 **Materials and Methods**

274 **Animals**

275 *Aeolosoma viride* was cultured in artificial spring water (ASW, 48 mg L^{-1} $NaHCO_3$,

276 24 mg L^{-1} $CaSO_4 \cdot 2H_2O$, 30 mg L^{-1} $MgSO_4 \cdot 7H_2O$, and 2 mg L^{-1} KCl in distilled water,

277 pH = 7.4) at 25°C under 12 hours of day-night cycles. Grounded oat meal serves as

278 major food source. Approximately 500 ± 200 worms were fed with 20 mg powdered

279 oats 3 to 5 times per week. Prior to all experiment, worms were starved in ASW

280 overnight.

281

282 **Regeneration experiment**

283 *Aeolosoma viride* without offspring was selected for the following experiment. To

284 analyze the capacity of regeneration, amputation was carried out at the desired

285 segment in *A. viride* (Fig. 1A). The detail morphological changes of regenerating

286 worms were observed with an Olympus DP80 microscope for the following 3 to 168

287 hours. The successful ratio of anterior or posterior regeneration was determined from

288 morphology and behavior with a dissecting microscope (WILD M8, Leica) at 1 to 7

289 days post-amputation (dpa).

290

291 In the inhibitory experiment, all procedures were similar as described earlier, but the

292 animal were transferred into fresh ASW containing 25 μM taxol (Sigma-Aldrich)

293

294 **EdU labeling**

295 Worms were treated with EdU (100 μg ml^{-1}) for 12 or 24 hours prior to amputation;

296 12 to 120 hours prior to fixation. The animals were fixed with 4% paraformaldehyde

297 (PFA) at 4□ overnight. Whole-mount immunohistochemistry detection was processed

298 using the Click-iT EdU Alexa Fluor 488 Imaging Kit (Invitrogen) according to the

299 manufacturer's protocol.

300

301 **RNA interference (RNAi)**

302 *Avi-tubulin* was cloned by our lab (NCBI # AQV09899.1). The RNA interference

303 protocol was modified as described previously [50]. Partial sequence of **y**ellow

304 fluorescent protein (*yfp*, as MOCK group) or *Avi-tubulin* were constructed with L4440

305 vector and transformed into an RNase III deficient strain competent cell HT115 (DE3)

306 (Yeastern Biotech). *A. viride* was fed with bacteria containing dsRNA for 3 days.

307

308 Microinjecting method was modified based on previous study [51]. The *yfp* or

309 *Avi-tubulin* dsRNA were *in vitro* transcribed with T7 polymerase (Ambion). Each
310 individual animal was injected 50 ng of dsRNA through microinjector (Promega) for
311 3 consecutive days. Worms were then collected for RNA extraction, protein extraction
312 or regeneration study afterward.
313
314 **RNA exaction and quantitative real-time RT-PCR (qRT-PCR)**
315 The total RNAs were extracted from 20 worms by using TRIzol and
316 thenreverse-transcribed to cDNA by using SuperScript III Kit (Invitrogen).
317 Transcriptional levels were determined by Bio-Rad iCycler™ (Bio-Rad) using SYBR
318 green system. The primers used to amplify *Avi-tubulin* were 5'-
319 GGTAACAACTGGGCTAAGGG-3' and 5'-GCGAAGCCAGGCATGAAGAA-3'.
320 *Avi-actin* was used as internal control with specific primers:
321 5'-ATGGAGAAGATCTGGCATCA-3' and 5'-GGAGTACTTGCGCTCAGGTG-3'
322 designed from *Avi-tublin* (NCBI # AQV09898.1). Relative quantification of gene
323 expression was calculated by using the ΔΔCt method. Three technical replicates were
324 used in each real-time PCR reaction, and a no-template blank was served as negative
325 control.
326
327 **Western blotting**

328 Animals were homogenized in RIPA buffer (50 mM Tris-HCl (pH 7.0), 150 mM NaCl,
329 1% Triton X-100, 0.5% $C_{24}H_{40}O_4$, 0.1% SDS with protease inhibitor cocktail
330 (Sigma-Aldrich) and DNase (Promega)). The homogenized samples were mixed with
331 sample buffer (60 mM Tris-HCl (pH 6.8), 25% glycerol, 2% SDS, 14.4 mM
332 2-mercaptoethanol and 0.1% bromophenol blue), separated by 7.5% polyacrylamide
333 gel, and transferred to a PVDF membrane (Millipore). After blocking with 5% BSA at
334 25□ for 1 h, the PVDF membrane was incubated with either anti-acetylated α-tubulin
335 (1:8000, GeneTex) or anti-α-actin (1:8000, Santa Cruz) antibodies in the blocking
336 solution at 25□ for 1 h, rinsed three times with PBST, and then incubated with either
337 HRP-conjugated goat anti-mouse IgG (1:3000, Chemicon-Millipore) for α-tubulin or
338 HRP-conjugated goat anti-rabbit IgG (1:8000, Chemicon-Millipore) for α-actin.
339 Finally, patterens were detected on the PVDF membrane by ECL (Bioman).
340

341 **Statistics**

342 Data were test for significance using one-way analysis of variance with a Scheffe's
343 method post *hoc* test or two-tailed unpaired student's t-test. Probability values of $p <$
344 0.05 were regarded as statistically significant.
345

346 **References**

1. Umesono Y, Tasaki J, Nishimura K, Inoue T, Agata K. Regeneration in an evolutionarily primitive brain--the planarian *Dugesia japonica* model. Eur J Neurosci 2011;34:863-9.

2. Watanabe H, Hoang VT, Mattner R, Holstein TW. Immortality and the base of multicellular life: Lessons from cnidarian stem cells. Semin Cell Dev Biol 2009;20:1114-25.

3. Gawriluk TR, Simkin J, Thompson KL, Biswas SK, Clare-Salzler Z, Kimani JM, Kiama SG, Smith JJ, Ezenwa VO, Seifert AW. Comparative analysis of ear-hole closure identifies epimorphic regeneration as a discrete trait in mammals. Nat Commun 2016;7:11164.

4. Morgan TH. Regeneration and liability to injury. Science 1901;14:235-48.

5. Agata K, Saito Y, Nakajima E. Unifying principles of regeneration I: epimorphosis versus morphallaxis. Dev Growth Differ 2007;49:73-8.

6. Maden M, Holder N. Axial characteristics of nerve induced supernumerary limbs in the axolotl. Wilehm Roux Arch Dev Biol 1984;193:394-401.

7. Reddien PW, Alvarado AS. Fundamentals of planarian regeneration. Annu Rev Cell Dev Biol 2004;20:725-57.

8. Passamaneck YJ, Martindale MQ. Cell proliferation is necessary for the regeneration of oral structures in the anthozoan cnidarian Nematostella vectensis.

366 BMC Dev Biol 2012;12:34.

367 9. Zattara EE, Bely AE. Evolution of a novel developmental trajectory: fission is

368 distinct from regeneration in the annelid *Pristina leidyi*. Evol Dev 2011;13:80-95.

369 10. Bely AE. Decoupling of fission and regenerative capabilities in an asexual

370 oligochaete. Hydrobiologia 1999;406:243-51.

371 11. Zattara EE, Bely AE. Investment choices in post-embryonic development:

372 quantifying interactions among growth, regeneration, and asexual reproduction in

373 the annelid *Pristina leidyi*. J Exp Zool B Mol Dev Evol 2013;320:471-88.

374 12. Zattara EE, Bely AE. Phylogenetic distribution of regeneration and asexual

375 reproduction in Annelida: regeneration is ancestral and fission evolves in

376 regenerative clades. Invertebr Biol 2016;135:400-14.

377 13. Bely AE. Early events in annelid regeneration: a cellular perspective. Integr Comp

378 Biol 2014;54:688-99.

379 14. Özpolat BD, Bely AE. Developmental and molecular biology of annelid

380 regeneration: a comparative review of recent studies. Curr Opin Genet Dev

381 2016;40:144-53.

382 15. de Jong DM, Seaver EC. Investigation into the cellular origins of posterior

383 regeneration in the annelid *Capitella teleta*. Regeneration (Oxf) 2018;5:61-77.

384 16. Bely AE, Wray GA. Evolution of regeneration and fission in annelids: insights

385 from *engrailed*- and *orthodenticle*-class gene expression. Development
386 2001;128:2781-91.
387 17. Glasby CJ, Timm T. Global diversity of polychaetes (Polychaeta; Annelida) in
388 freshwater. Hydrobiologia 2008;595:107-15.
389 18. Falconi R, Gugnali A, Zaccanti F. Quantitative observations on asexual
390 reproduction of *Aeolosoma viride* (Annelida, Aphanoneura). Invertebr Biol
391 2015;134:151-61.
392 19. Herlant-Meewis H. Contribution a l'étude de la régénération chez les oligochètes
393 Aeolosomatidae. Ann Soc r Zool Belg 1953;84:117-61.
394 20. Bradshaw B, Thompson K, Frank U. Distinct mechanisms underlie oral vs aboral
395 regeneration in the cnidarian *Hydractinia echinata*. Elife 2015;4:e05506.
396 21. de Lucas B, Pérez LM, Gálvez BG. Importance and regulation of adult stem cell
397 migration. J Cell Mol Med 2017;22:746-54.
398 22. Myohara M, Yoshida-Noro C, Kobari F, Tochinai S. Fragmenting oligochaete
399 *Enchytraeus japonensis*: a new material for regeneration study. Dev Growth
400 Differ 1999;41:549-55.
401 23. Xiao N, Ge F, Edwards CA. The regeneration capacity of an earthworm, *Eisenia*
402 *fetida*, in relation to the site of amputation along the body. Acta Ecologica Sinica
403 2011;31:197-204.

404 24. Balavoine G. Segment formation in annelids: patterns, processes and evolution.
405 Int J Dev Biol 2014;58:469-83.
406 25. Bely AE. Distribution of segment regeneration ability in the Annelida. Integr
407 Comp Biol 2006;46:508-18.
408 26. Nechiporuk A, Keating MT. A proliferation gradient between proximal and
409 *msxb*-expressing distal blastema directs zebrafish fin regeneration. Development
410 2002;129:2607-17.
411 27. Schnapp E, Kragl M, Rubin L, Tanaka EM. Hedgehog signaling controls
412 dorsoventral patterning, blastema cell proliferation and cartilage induction during
413 axolotl tail regeneration. Development 2005;132:3243-53.
414 28. de Jong DM, Seaver EC. A stable thoracic *Hox* code and epimorphosis
415 characterize posterior regeneration in *Capitella teleta*. PLoS One
416 2016;11:e0149724.
417 29. Licciano M, Murray JM, Watson GJ, Giangrande A. Morphological comparison of
418 the regeneration process in *Sabella spallanzanii* and *Branchiomma luctuosum*
419 (Annelida, Sabellida). Invertebr Biol 2012;131:40-51.
420 30. Cai SA, Fu X, Sheng Z. Dedifferentiation: a new approach in stem cell research.
421 BioScience 2007;57:655-62.
422 31. Kalidas RM, Raja SE, Mydeen SAKNM, Samuel SCJR, Durairaj SCJ, Nino GD,

423 Palanichelvam K, Vaithi A, Sudhakar S. Conserved lamin A protein expression in
424 differentiated cells in the earthworm *Eudrilus eugeniae*. Cell Biol Int
425 2015;39:1036-43.
426 32. Kozin VV, Kostyuchenko RP. *Vasa*, *PL10*, and *Piwi* gene expression during caudal
427 regeneration of the polychaete annelid Alitta virens. Dev Genes Evol
428 2015;225:129-38.
429 33. Martinez VG, Reddy PK, Zoran MJ. Asexual reproduction and segmental
430 regeneration, but not morphallaxis, are inhibited by boric acid in *Lumbriculus*
431 *variegatus* (Annelida: Clitellata: Lumbriculidae). Hydrobiologia 2006;564:73-86.
432 34. Özpolat BD, Bely AE. Gonad establishment during asexual reproduction in the
433 annelid *Pristina leidyi*. Dev Biol 2015;405:123-36.
434 35. Tweeten KA, Anderson A. Analysis of cell proliferation and migration during
435 regeneration in *Lumbriculus variegatus* (Clitellata: Lumbriculidae). BIOS
436 2008;79:183-90.
437 36. Aboobaker AA. Planarian stem cells: a simple paradigm for regeneration. Trends
438 Cell Biol 2011;21:304-11.
439 37. Gentile L, Cebria F, Bartscherer K. The planarian flatworm: an *in vivo* model for
440 stem cell biology and nervous system regeneration. Dis Model Mech
441 2011;4:12-9.

442 38. Umesono Y, Agata K. Evolution and regeneration of the planarian central nervous
443 system. Dev Growth Differ 2009;51:185-95.
444 39. Galliot B. Hydra, a fruitful model system for 270 years. Int J Dev Biol
445 2012;56:411-23.
446 40. Park HD, Ortmeyer AB, Blankenbaker DP. Cell division during regeneration in
447 *Hydra*. Nature 1970;227:617-9.
448 41. Dübel S, Schaller HC. Terminal differentiation of ectodermal epithelial stem cells
449 of *Hydra* can occur in G2 without requiring mitosis or S phase. The Journal of
450 Cell Biology 1990;110:939-45.
451 42. Chiu H, Alqadah A, Chuang CF, Chang C. *C. elegans* as a genetic model to
452 identify novel cellular and molecular mechanisms underlying nervous system
453 regeneration. Cell Adh Migr 2011;5:387-94.
454 43. Endo T, Bryant SV, Gardiner DM. A stepwise model system for limb regeneration.
455 Dev Biol 2004;270:135-45.
456 44. Worley MI, Setiawan L, Hariharan IK. Regeneration and transdetermination in
457 *Drosophila* imaginal discs. Annu Rev Genet 2012;46:289-310.
458 45. Dubois P, Ameye L. Regeneration of spines and pedicellariae in echinoderms: a
459 review. Microsc Res Tech 2001;55:427-37.
460 46. Yu N, Christiaens O, Liu J, Niu J, Cappelle K, Caccia S, Huvenne H, Smagghe G.

461 Delivery of dsRNA for RNAi in insects: an overview and future directions. Insect
462 Sci 2013;20:4-14.
463 47. Canistro D, Boccia C, Falconi R, Bonamassa B, Valgimigli L, Vivarelli F, Soleti A,
464 Genova ML, Lenaz G, Sapone A, et al. Redox-based flagging of the global
465 network of oxidative stress greatly promotes longevity. J Gerontol A Biol Sci
466 Med Sci 2015;70:936-43.
467 48. Falconi R, Renzulli T, Zaccanti F. Survival and reproduction in *Aeolosoma viride*
468 (Annelida, Aphanoneura). Hydrobiologia 2006;564:95-9.
469 49. Nandini S, Sarma SSS. Effect of *Aeolosoma* sp. (Aphanoneura: Aeolosomatidae)
470 on the population dynamics of selected cladoceran species. Hydrobiologia
471 2004;526:157-63.
472 50. Kamath RS, Martinez-Campos M, Zipperlen P, Fraser AG, Ahringer J.
473 Effectiveness of specific RNA-mediated interference through ingested
474 double-stranded RNA in *Caenorhabditis elegans*. Genome Biol
475 2001;2:research0002.1-research.10.
476 51. Newmark PA, Reddien PW, Cebrià F, Alvarado AS. Ingestion of bacterially
477 expressed double-stranded RNA inhibits gene expression in planarians. Proc Natl
478 Acad Sci U S A 2003;100:11861-5.
479

Acknowledgments

We thank Dr. Kuo Dian-Han and Dr. Lai Yi-Te, who contributed greatly by proving continual guidance, editing and reviewing this manuscript.

Funding

This study was supported in part by a grant from the Ministry of Science and Technology (MOST, Taiwan, grant no. 103-2311-B-002-017-MY3)

Availability of data and materials

The datasets generated and/or analysed during the current study are available from the corresponding author on reasonable request.

Author contributions

All authors designed the experiments. CC, SF and YH carried out the experiments. CC and SF interpreted the data. CC and SF wrote the manuscript. JC reviewed this manuscript.

Competing interests

The authors declare no competing interests.

Figure legends

Figure 1. The morphology and paratonic fission of intact *A. viride*. (A) The first segment of intact *A. viride* has a prostomium and a peristomium with a mouth. Average *A. viride* contains 10 to 12 segments with pairs of chaetae. The transparent body has an enlarged digestive tract located at the center of its body. The pygidium is located on the last segment of the posterior end. The red dashed line indicated the amputation site in front of enlarged digestive tract. (B) After the worm was amputated at the site indicated in (A), the two fragments will individually proceed anterior or posterior regeneration (indicated by white arrows). (C-E) The process of paratonic fission separated an intact worm into two individuals. Worms with unusual lengthy posterior region could be easily observed (Fig. 1C). The anterior portion of the offspring gradually developed, and tilted apart from the parental worm (Fig. 1D). The offspring worm break apart from the parental worm, and become an individual worm (Fig. 1E). The white arrow indicated interface between parent and offspring worm. Scale bar: 1 mm.

Figure 2. Anterior regeneration in *A. viride*. The worms were amputated in front of the enlarged digestive tract, and the external morphology was observed in intact (A)

518 and 0 to 120 hpa (B) during regeneration. The intact worm has a mouth that can be
519 observed at both dorsal and ventral side of the peristomium at the first segment.
520 During anterior regeneration, the rough wounded area became smooth during wound
521 closure within 3 to 6 hpa. The protruding regenerative blastema became apparent from
522 24 to 48 hpa in most regenerating *A. viride*. Mouth formation, could be observed
523 around 96 hpa. After 96 hours of regeneration, the cephalic shape started to bulging.
524 Then, the prostomium expanded from 96 to 120 hpa. The amputation site was labeled
525 by black dotted line and the black arrow indicated the re-opening of mouth. Scale bar:
526 50 μm.
527
528 **Figure 3. Minimum segments required for successful regeneration in *A. viride*.**
529 Worms were amputated into different number of segments. The successful ratio of
530 either anterior or posterior regeneration in amputated worms regenerating from
531 different segments were observed at 5 or 3 dpa. The minimum segments required for
532 successful regeneration in *A. viride* was 3. All data represented the mean ± s.d. from
533 at least three independent duplicate experiments (n = 10). One-way ANOVA was
534 performed to determine the significance of success rates compared to each group. *: p
535 <0.05; **: $p < 0.01$.
536

537 **Figure 4. Cell proliferation was detected by EdU labeling during anterior**
538 **regeneration in *A. viride*.** Worms were incubated in 100 μg ml^{-1}EdU for 12 hours
539 prior to collecting the specimen at different time points after amputation. (A) EdU
540 signal (green) reveals cell proliferation conformed by nuclei stained with Hoechst
541 33342 (blue). The white dotted line indicates the colocalization cells in three channels.
542 Scale bar: 10 μm. (B) The worms were labeled with Hoechst 33342 and EdU in intact
543 worm. Figure on the right were magnified pictures of the head or tail regions. The
544 yellow arrow indicates the asexual reproductive zone. Since the asexual reproductive
545 zone undergo continued cell proliferation to produce progeny, the area showed
546 stronger signal of Hoechst 33342 which indicates the presence of larger amount of
547 cells. H: head, T: tail. (C) Cell proliferation was detected on anterior regenerating site
548 at different time points. Prior to amputation, the head, mouth showed the strongest
549 EdU signal. Minor proliferating cells randomly distributed throughout the body. After
550 12 hpa, EdU signal became focused at the wounded site. Edu signal completely
551 diminished post the amputation site after 24 hpa. The EdU signal peaked at 24 and 48
552 hpa, then gradually diminished. The amputation site is labeled by yellow dotted line.
553 Red triangle indicated the reappeared mouth. Scale bar: 100 μm.
554
555 **Figure 5. The inhibitory effect of taxol on cell proliferation and anterior**

regeneration in *A. viride*. (A) *A. viride* weas incubated in EdU 12 hours prior to fixation at 48 hpa. The amount of proliferating cells at the blastema was decreased after 25 μM taxol treatment. (B, C) The regeneration successful ratio was examined from 1 to 7 dpa. Taxol treated worms showed delay and significant decrease compare to the control group at 7 dpa. (D) The head morphology of regenerating worms was obviously affected by taxol treatment. Head formation could be clearly observed in regenerating worm incubated in 0.5% ethanol at 5 dpa, however, only a piece of protruding tissue could be observed in the taxol treated group. At 7 dpa, the ethanol treated group demonstrated normal regeneration, but the taxol treated group barely started the formation of a regenerative blastema. Scale bar: 100 μm. All data represented the mean ± s.d. from at least three independent duplicate experiments. Significant differences relative to control group (0.5% etanol) were denoted by *. *: p <0.05; **: $p < 0.01$; ***: $p < 0.001$ using two-tailed unpaired student's t-test.

Figure 6. The inhibitory effect of *Avi-tubulin* microRNA on anterior regeneration. Either the expression level of *Avi-tublin* mRNA (A) or protein (B) expression levels o were detected to assay the knock-down efficiency. The inhibitory effect of regeneration successful ratio by *Avi-tubulin* RNAi was observed at 120 hpa (C). One-way ANOVA was performed to determine the significance of mRNA, protein

575 expression or successful ratio compared to control group. **: $p < 0.01$.

576

577 **Figure 7. Limited cell migration is observed at anterior regenerating site of *A.***

578 ***viride*.** The proliferating cells were incorporated by EdU for 24 hours prior to

579 amputation in intact and regenerating worms. At 24, 72, 120 hours post amputation,

580 minor EdU^+ cell migrated to regenerating area. Although limited signals could be

581 detected at the surface of regenerating worms, the number of proliferating cells

582 significantly differed from the area behind amputation site. The white dotted line

583 indicates the reappearance of enlarged head. The yellow bracket indicated the

584 enlarged area for the figure on the right side. Scale bar: 100 μm.

Figure 1

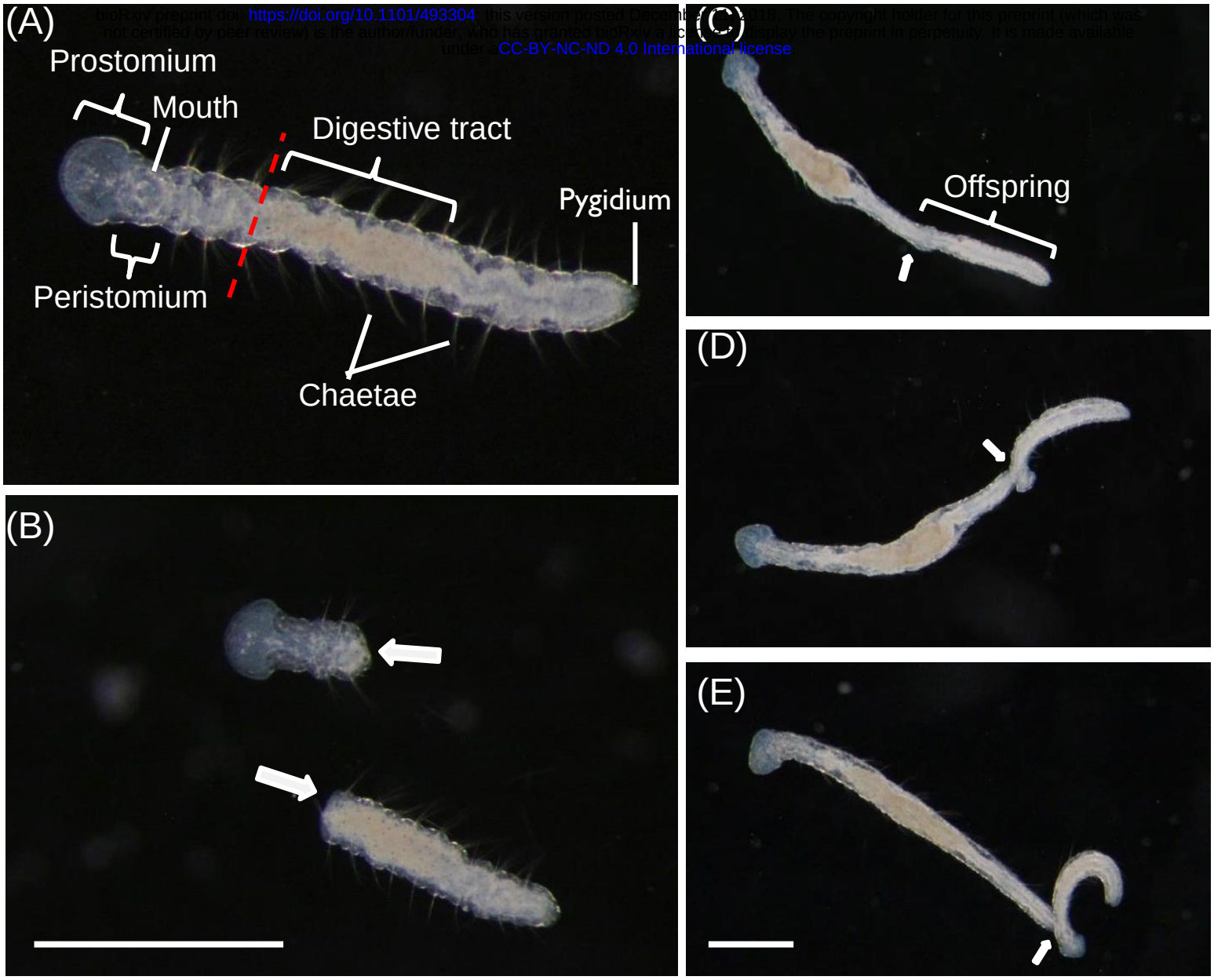

Figure 2

(A)

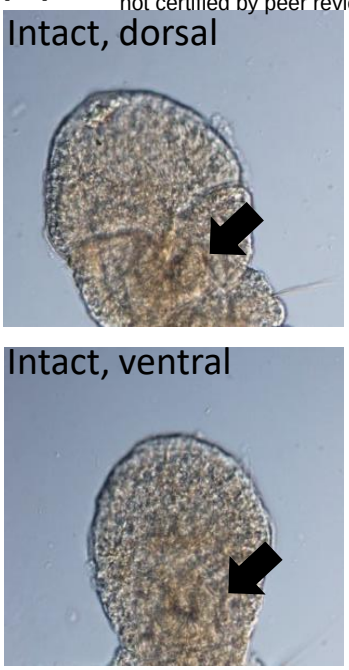

(B)

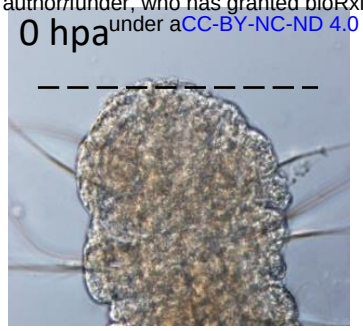

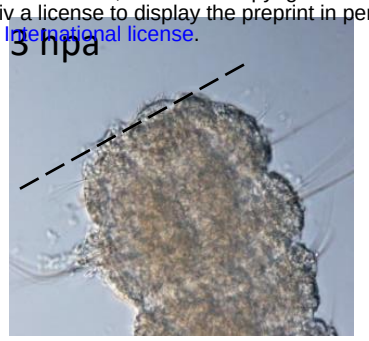

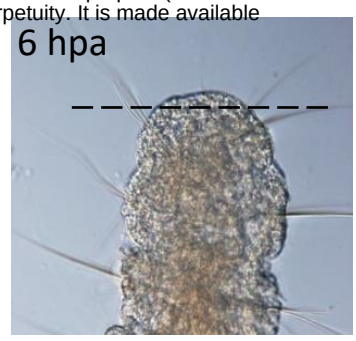

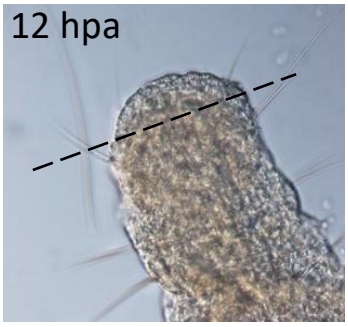

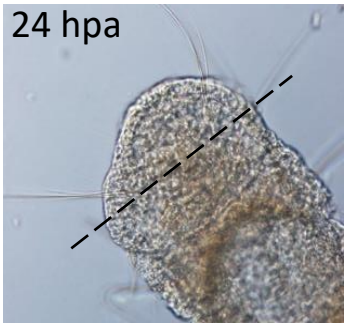

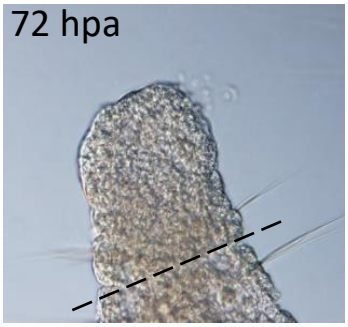

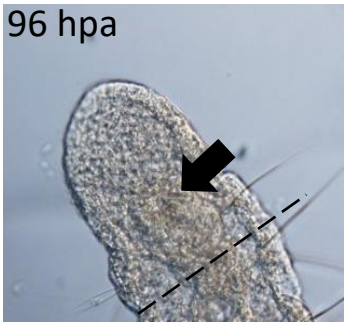

Figure 3

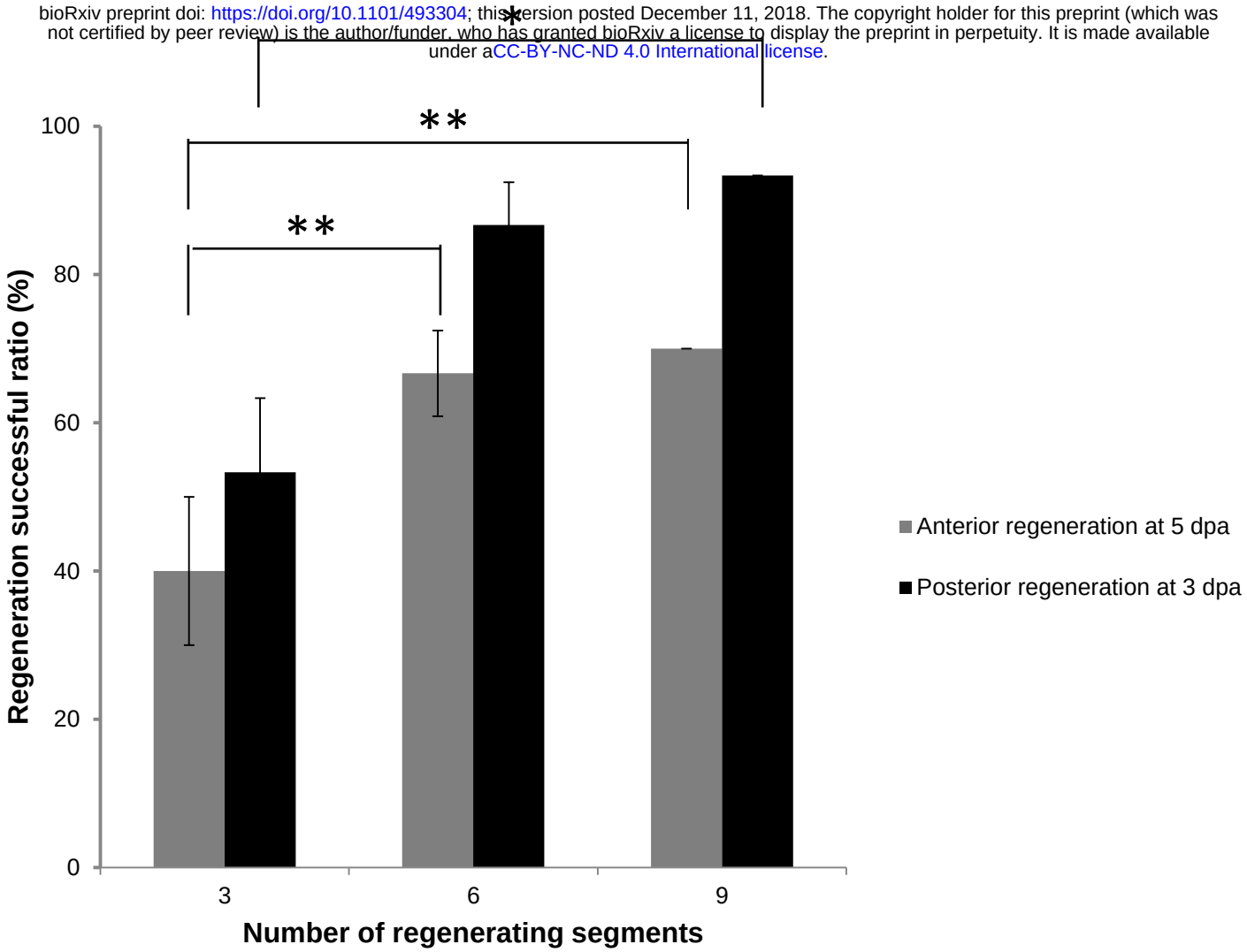

Figure 4

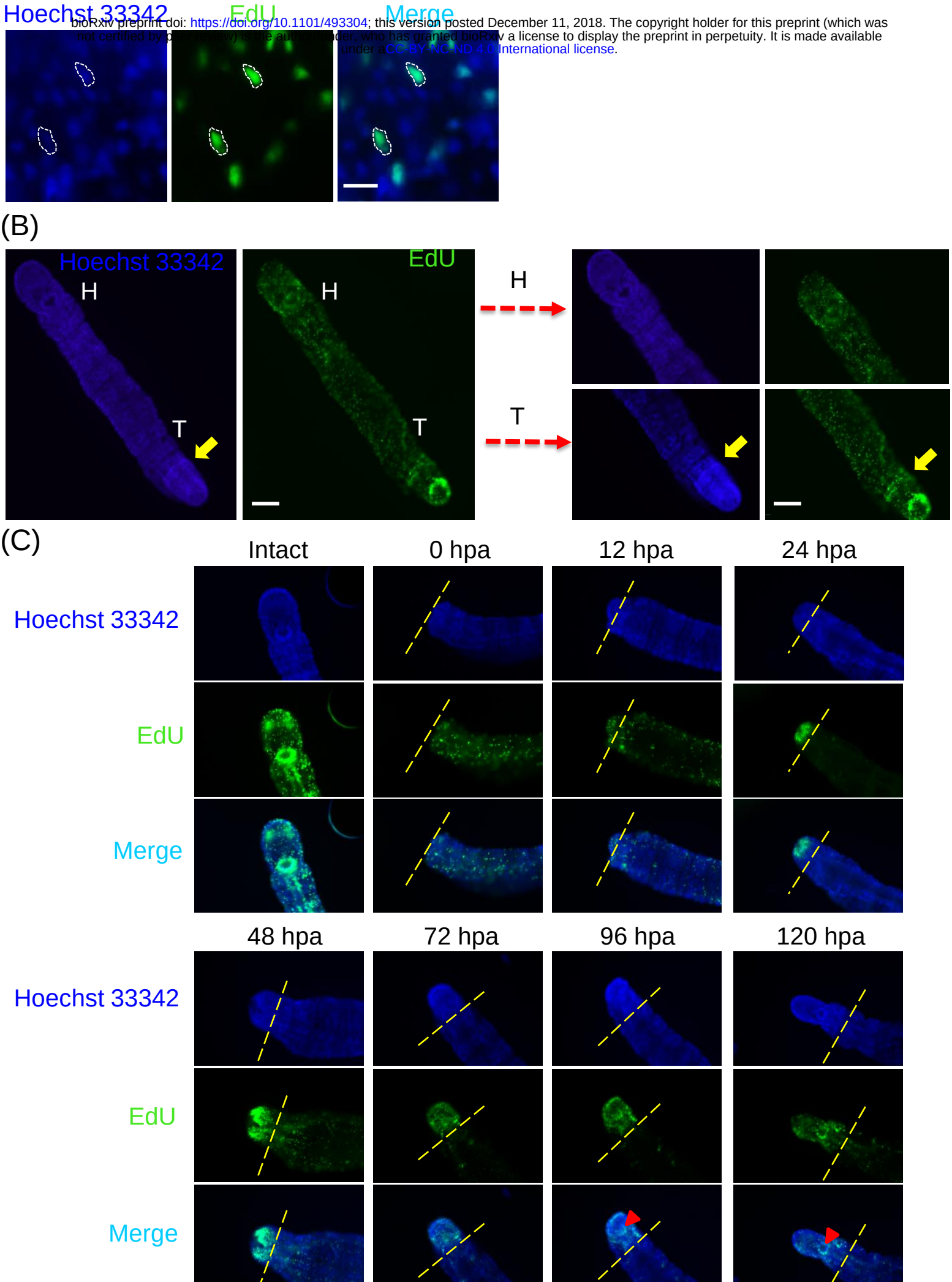

Figure 5

(A)

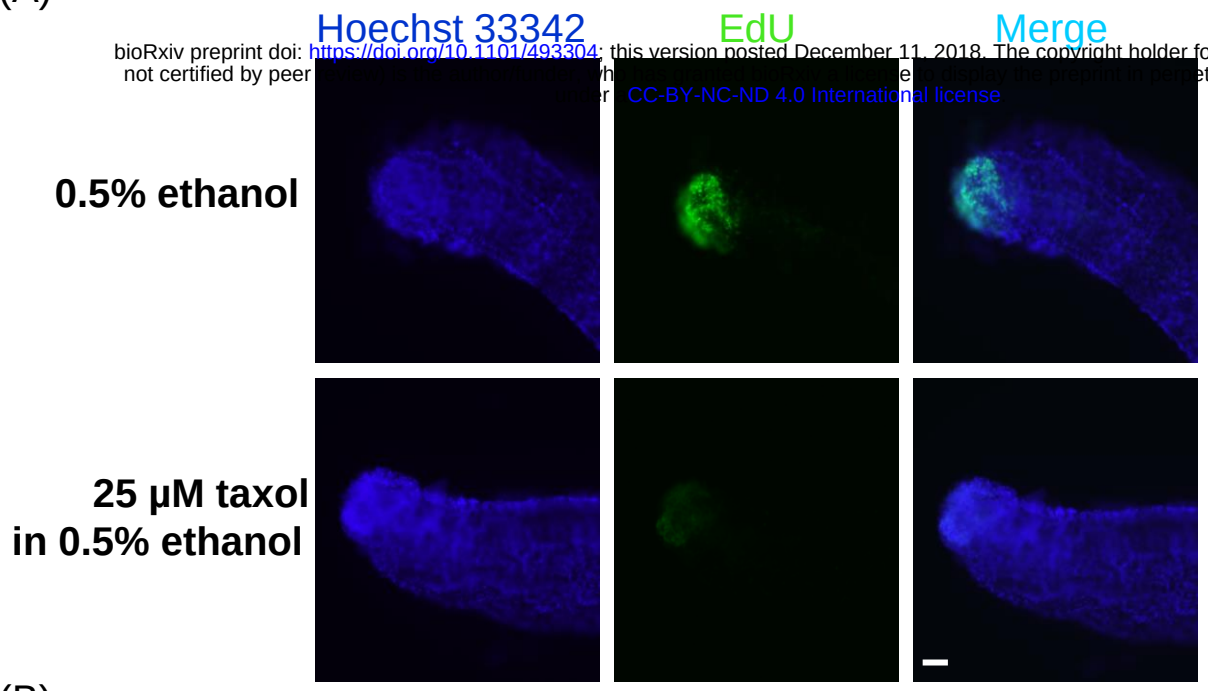

(B)

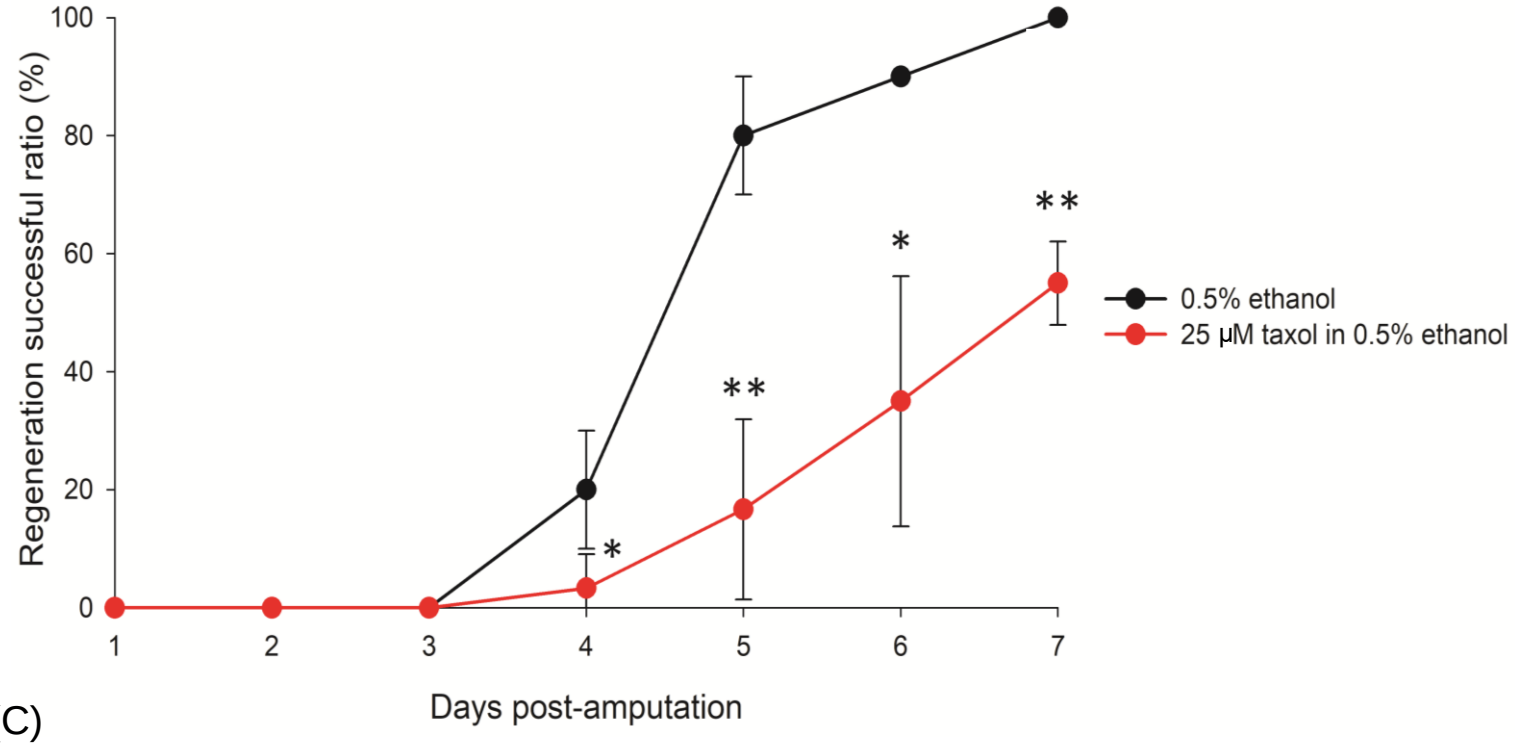

(C)

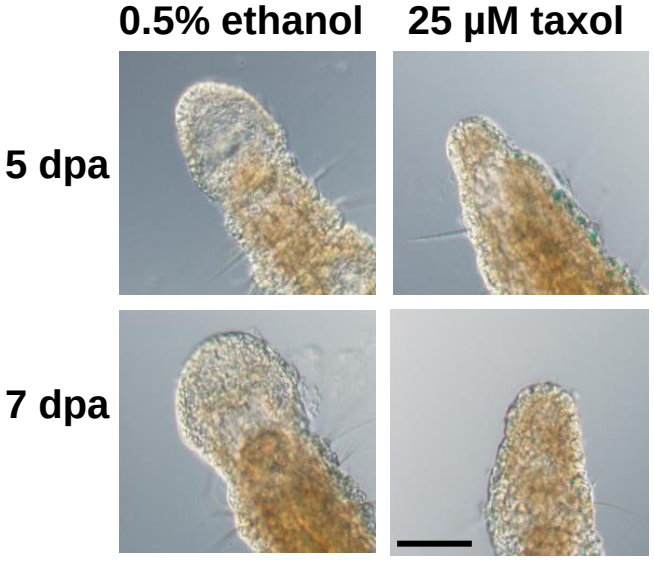

Figure 6

(A)

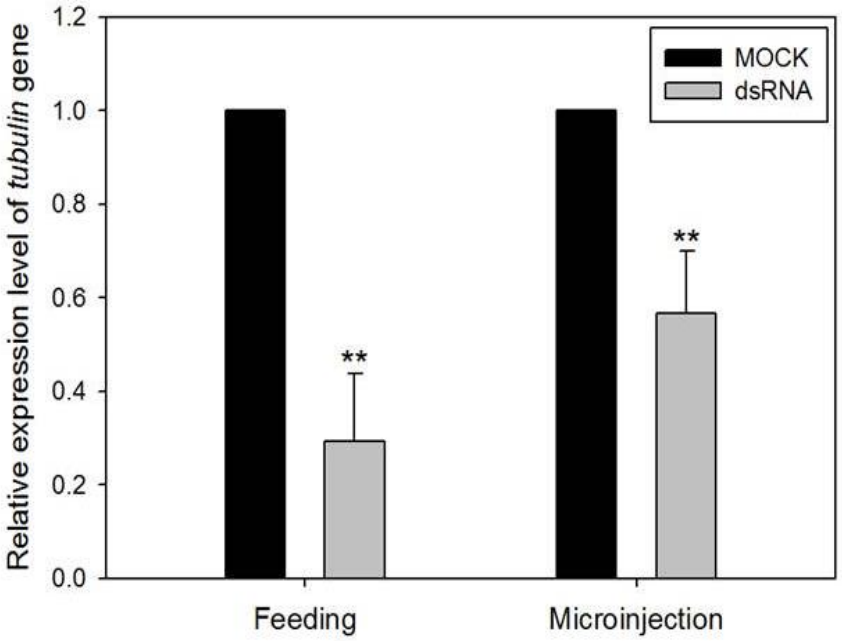

(B)

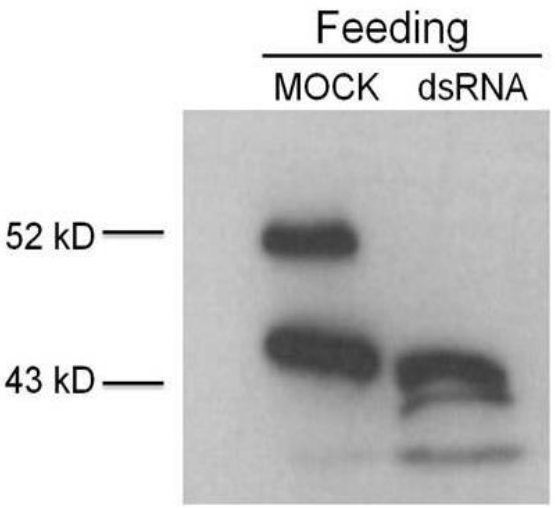

(C)

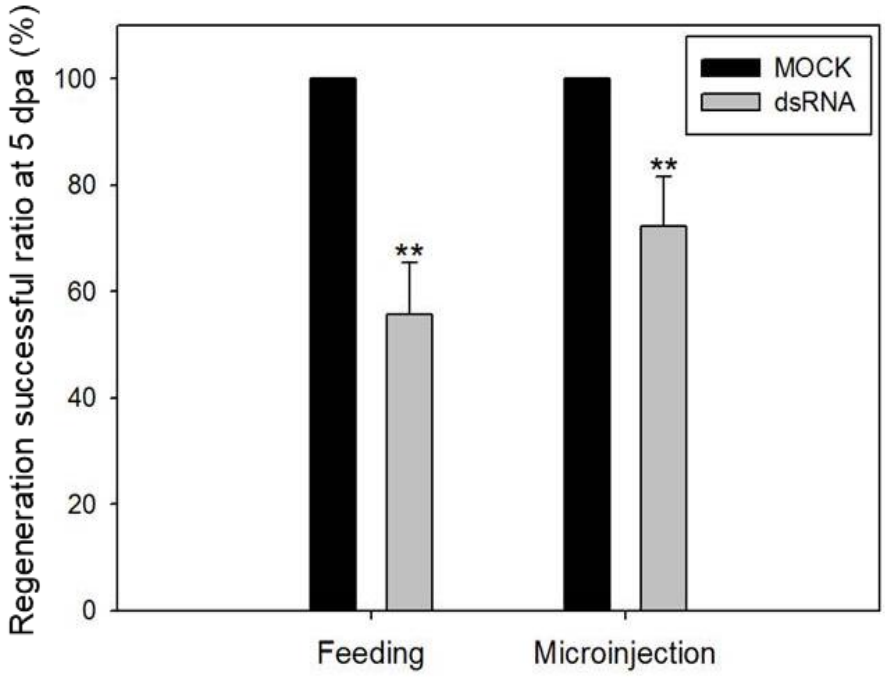

Figure 7